Electronic Supplementary Material (ESI) for CrystEngComm

Electronic Supplementary Information

Nanocrystalline Diamond Microstructures from $Ar/H_2/CH_4$-plasma Chemical Vapour Deposition

*I-Nan Lin, Huang-Chin Chen, Chuang-Shern Wang, Yun-Rue Lee, and Chi-Young Lee**

(a) polymorphs of tetrahedral bonded carbons

To understand the nature of the defects observed in Fig. 5, the structure of the polymorphs of diamond materials was re-investigated. Figs. S1a and S1b illustrate, the [111] projection of face-centered cubic (fcc) lattices and [0001] projection of hexagonal-close-packed (hcp) lattices respectively. These figures clearly shows the first 3 layers of atoms sequentially stacked in these lattices, in white, grey and black spheres, respectively. It should be noted that, in fcc-lattices, the atoms in the third layer (black spheres) are sitting at the locations different from those in layers A (white spheres) or B (grey spheres), resulting in a sequence ABCABC…. In contrast, the atoms in the third layer of hcp-lattices (black spheres) are sitting at the same locations as those in layer A (white spheres), resulting in ABABAB…stacking sequence. The 3C cubic diamond lattices and 2H-hexagonal diamond lattices can be derived from the fcc- and hcp-lattices respectively, by replacing the carbons for the atoms at the 4 apexes of each tetrahedrons shown in Fig. S1 and at the same time, inserting a carbon atom into each tetrahedrons. The atomic arrangement of carbon atoms for the 3C-lattices viewed along $[20\bar{2}]$ direction is more clearly illustrated in Fig. S2a. The simulated structure image (by JEMS package, Joel) is shown in Fig. S2b along with the simulated electron diffraction (simulated ED, inset). On the other hand, the stacking sequence of carbon atoms for the 2H-lattices viewed along $2\bar{1}\bar{1}0$ zone axis is illustrated in Fig. S2c. The simulated structure image (JEMS package, Joel) is shown in Fig. S2d, along with the corresponding simulated ED (inset).

In addition to the ABABAB…stacking sequence for 2H-diamonds, there are other forms of polymorphs, which have low formation energy and possess large probability to occur. These polymorphs are summarized in Fig. S3 for the stacking sequences of the 4H, 6H, 8H, 15R and 21R hexagonal lattices, viewed along $2\bar{1}\bar{1}0$ zone axis. The structure image of $2\bar{1}\bar{1}0$ zone axis nH-diamond lattices (simulated by JEMS package, Joel), are shown in Fig. S4, along with the corresponding simulated ED. These figures show that the crystalline symmetry of the materials can be easily differentiated from the SAED in $2\bar{1}\bar{1}0$ zone axis. Comparing the planar defects shown in Figs. 6a and 6b with the simulated structural images and ED in Fig. S4, the planar defects C and D can be assigned as 8H-diamonds. It should be noted that other forms of isomorphism of diamond may also occurred in these samples. But the structural images of these isomorphisms are very similar with those of 2H structure image and cannot be clearly resolved.

In 3C-diamond crystal, a characteristic of planar stacking fault will be observed, if one of the (111) layer was misplaced, either as a missing plane (ABC“ • ”BCAB…) or an extra plane (ABC“B”ABC…). In this case, streaks lying along [111] direction will be observed, associating with all the major diffraction spots. Such kind of images was observed in the region B in Fig. 5b. On the other hand, a characteristic of two-phase materials will be observed if nH-lattices are of considerable thickness. This is the case illustrated in regions C and D in Fig. 5d.

(b) TEM microstructure of $UNCD_{10}$ films:

TEM micrograph in Fig. 3b shows that $UNCD_{10}$ films contain dendrite-like granular structure, which is significantly different from the elongated geometry for the $UNCD_{01}$ films. To illustrate that even though the

appearance of the microstructure of the two films looks different, they are actually formed by the same pathway, the detail microstructure of the $UNCD_{10}$ films are shown in Fig. S5. Fig. S5a shows one of the typical dendrite-like grains, which are about 200×600 nm in size. The SAED shown as inset in Fig. S5a indicates again there contains rel-rods passing through each major diffraction spots, which implies that the dendrite-like grains contain planar defects (stacking faults). Fig. S5b shows the TEM structure image of the region designated in Fig. S5a, indicating that the granular structure is also very complicated. However, enlarged structure image for the region designated is shown in Fig. S5c. This micrograph reveals that the area 1 is stacking fault, which is similar to those in Fig. 8b for $UNCD_{01}$ films, whereas area 2 is hexagonal diamond, which is similar to those in Fig. 5d for MCD_{75} films.

Apparently, although the relative proportion of the defects, stacking faults and hexagonal diamond, occurred in $UNCD_{10}$ films is different from that in $UNCD_{01}$ or MCD_{75} films, they are essential of the same nature. The implication of such an observation is that although the plasma for growing $UNCD_{10}$ films is different from those for synthesizing $UNCD_{01}$ or MCD_{75} films, the reaction occurred near the surface of diamond films are essentially the same. The granular structure was formed by similar sequences: (i) the encapsulation of newly formed diamond clusters by hydrocarbon, (ii) secondary nucleation, (iii) re-activation of hydrocarbon by atomic hydrogen in the plasma and (iv) enlargement of diamond grains via the attachment of active carbon species in the plasma. The final microstructure is resultant of the competition of these processing steps.

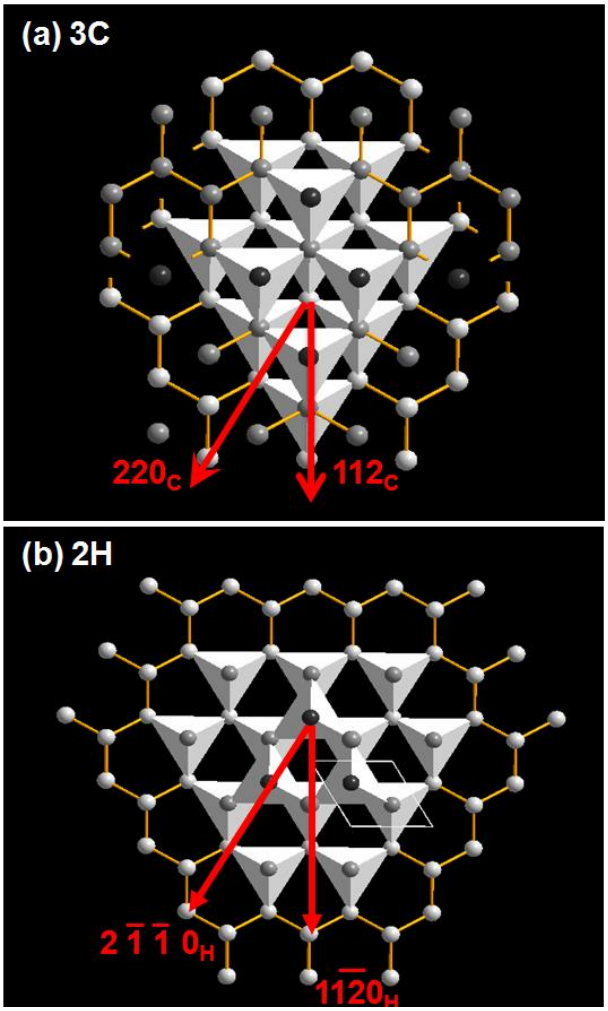

Fig. S1 The schematics of the arrangement of carbon atoms: (a) [111] projection of cubic diamond structure and (b) [0001] projection of hexagonal diamond structure.

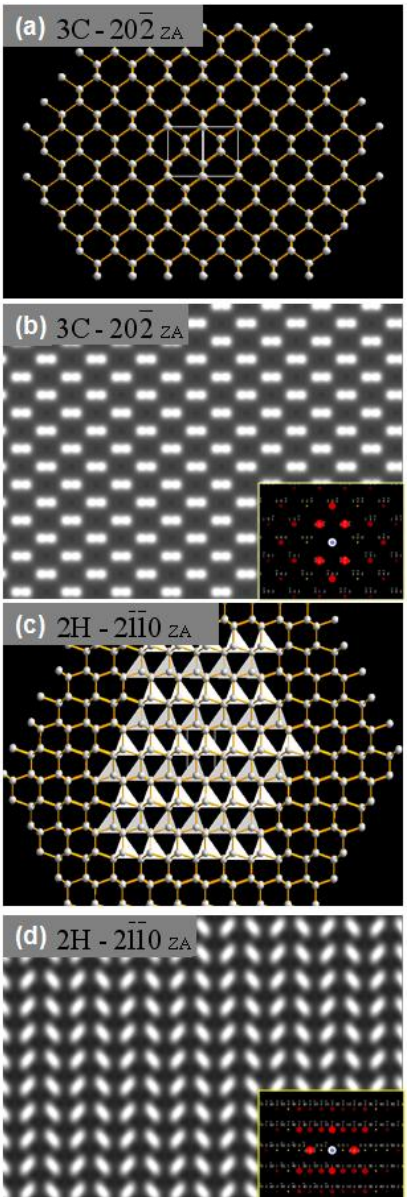

Fig. S2 The schematics of (a) the arrangement of carbon atoms viewed along 220 zone axis for 3C cubic diamond structure and (b) the structure image of 3C-lattices simulated by JEMS package (Joel); with the inset showing the simulated ED. The schematics of (c) the arrangement of carbon atoms viewed along $2\bar{1}\bar{1}0$ zone axis for 2H hexagonal diamond structure and (d) the structure image of 2H-lattices simulated by JEMS package (Joel), with the inset showing the simulated ED.

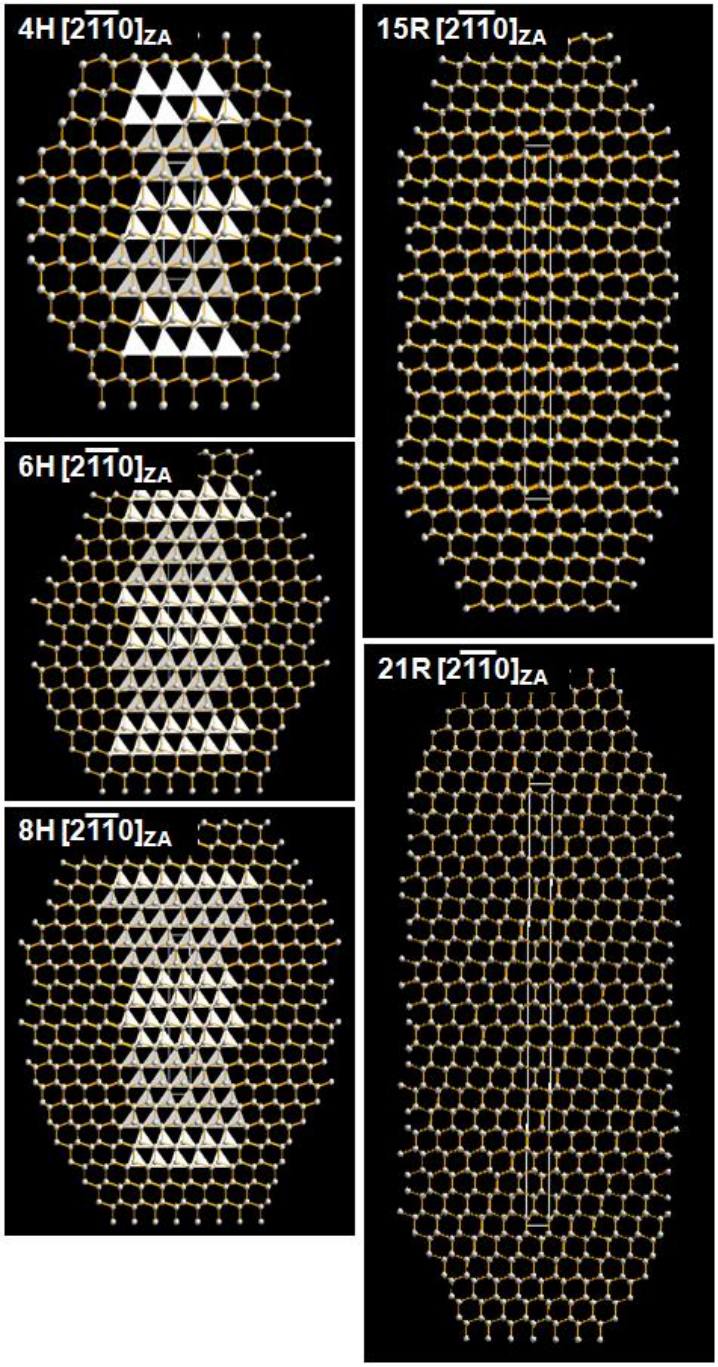

Fig. S3 The schematics of the arrangement of carbon atoms for 4H, 6H, 8H 15R and 21R isomorphism of diamond structure.

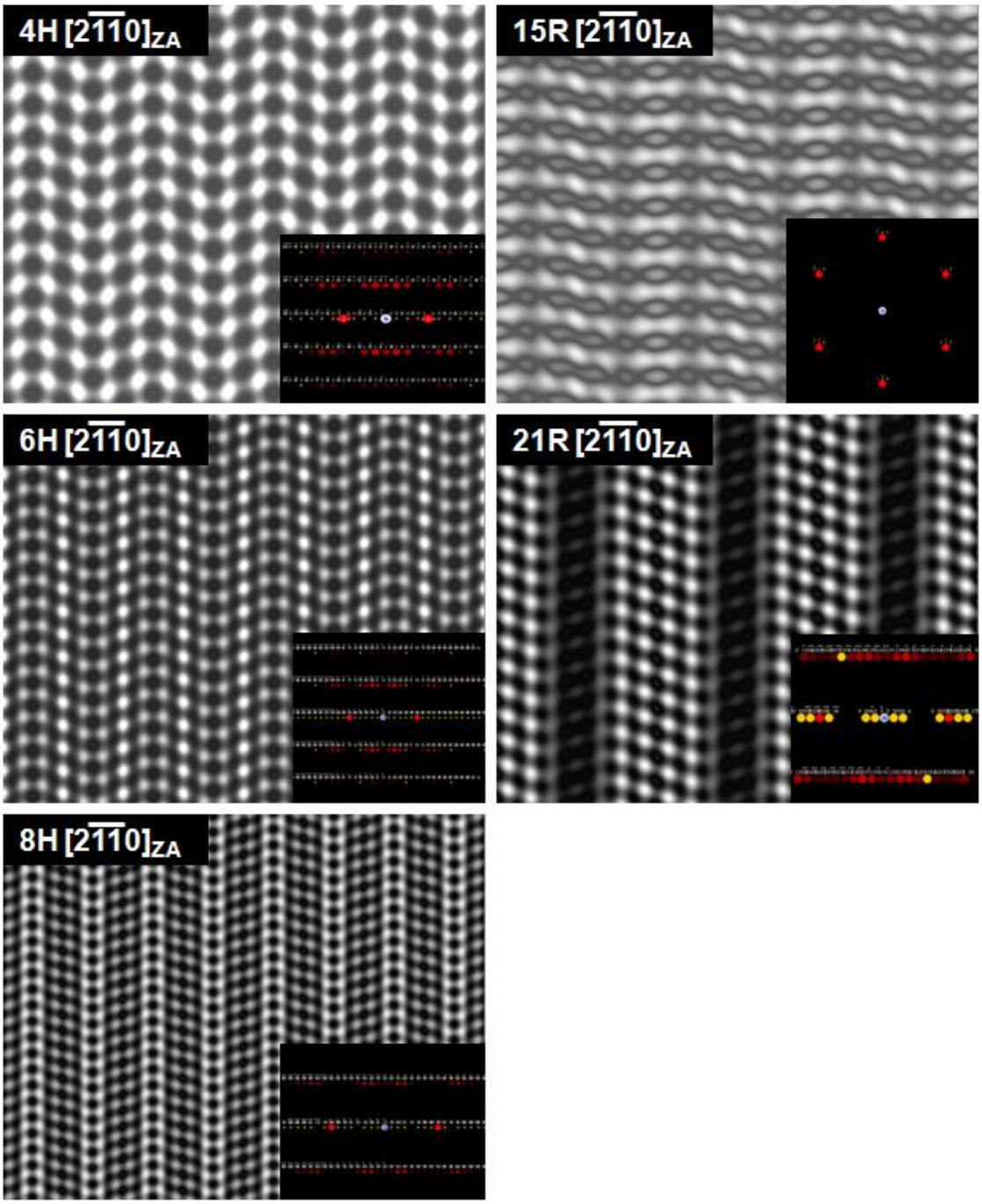

Fig. S4 The structure image simulated by JEMS package (Joel), with the inset showing the simulated ED for 4H, 6H, 8H 15R and 21R isomorphism of diamond structure.

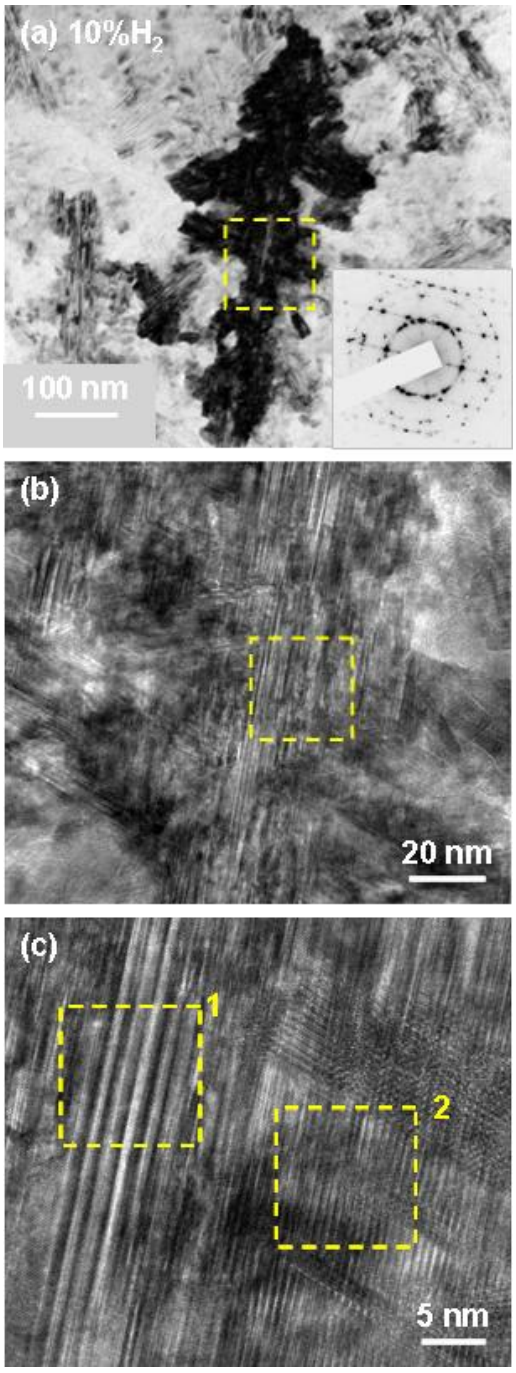

Fig. S5 The (a) bright field TEM micrograph, (b) structure image of the region designated in "a" and (c) structure image of the area designated in "b".